## Supplementary data

**Coding nucleotide sequence of F8-VEGF-C**

GAGGTGCAGCTGTTGGAGTCTGGGGGAGGCTTGGTACAGCCTGGGGGGTCCCTGAGA
CTCTCCTGTGCAGCCTCTGGATTCACCTTTAGCCTGTTTACGATGAGCTGGGTCCGCC
AGGCTCCAGGGAAGGGGCTGGAGTGGGTCTCAGCTATTAGTGGTAGTGGTGGTAGCA
CATACTACGCAGACTCCGTGAAGGGCCGGTTCACCATCTCCAGAGACAATTCCAAGA
ACACGCTGTATCTGCAAATGAACAGCCTGAGAGCCGAGGACACGGCCGTATATTACT
GTGCGAAAAGTACTCATTTGTATCTTTTTGACTACTGGGGCCAGGGAACCCTGGTCA
CCGTCTCGAGTGGCGGTAGCGGAGGGGAAATTGTGTTGACGCAGTCTCCAGGCACCC
TGTCTTTGTCTCCAGGGGAAAGAGCCACCCTCTCCTGCAGGGCCAGTCAGAGTGTTAG
CATGCCGTTTTTAGCCTGGTACCAGCAGAAACCTGGCCAGGCTCCCAGGCTCCTCATC
TATGGTGCATCCAGCAGGGCCACTGGCATCCCAGACAGGTTCAGTGGCAGTGGGTCT
GGGACAGACTTCACTCTCACCATCAGCAGACTGGAGCCTGAAGATTTTGCAGTGTAT
TACTGTCAGCAGATGCGTGGTCGGCCGCCGACGTTCGGCCAAGGGACCAAGGTGGAA
ATCAAATCTTCCTCATCGGGTAGTAGCTCTTCCGGCTCATCGTCCAGCGGCGCACATT
ATAATACAGAGATCTTGAAAAGTATTGATAATGAGTGGAGAAAGACTCAATGCATGC
CACGGGAGGTGTGTATAGATGTGGGGAAGGAGTTTGGAGTCGCGACAAACACCTTCT
TTAAACCTCCATGTGTGTCCGTCTACAGATGTGGGGGTTGCTGCAATAGTGAGGGGC
TGCAGTGCATGAACACCAGCACGAGCTACCTCAGCAAGACGTTATTTGAAATTACAG
TGCCTCTCTCTCAAGGCCCCAAACCAGTAACAATCAGTTTTGCCAATCACACTTCCTG
CCGATGCATGTCTAAACTGGATGTTTACAGACAAGTTCATTCCATTATTAGACGT

**Coding nucleotide sequence of F8-VEGF-C156Ser**

GAGGTGCAGCTGTTGGAGTCTGGGGGAGGCTTGGTACAGCCTGGGGGGTCCCTGAGA
CTCTCCTGTGCAGCCTCTGGATTCACCTTTAGCCTGTTTACGATGAGCTGGGTCCGCC
AGGCTCCAGGGAAGGGGCTGGAGTGGGTCTCAGCTATTAGTGGTAGTGGTGGTAGCA
CATACTACGCAGACTCCGTGAAGGGCCGGTTCACCATCTCCAGAGACAATTCCAAGA
ACACGCTGTATCTGCAAATGAACAGCCTGAGAGCCGAGGACACGGCCGTATATTACT
GTGCGAAAAGTACTCATTTGTATCTTTTTGACTACTGGGGCCAGGGAACCCTGGTCA
CCGTCTCGAGTGGCGGTAGCGGAGGGGAAATTGTGTTGACGCAGTCTCCAGGCACCC
TGTCTTTGTCTCCAGGGGAAAGAGCCACCCTCTCCTGCAGGGCCAGTCAGAGTGTTAG
CATGCCGTTTTTAGCCTGGTACCAGCAGAAACCTGGCCAGGCTCCCAGGCTCCTCATC
TATGGTGCATCCAGCAGGGCCACTGGCATCCCAGACAGGTTCAGTGGCAGTGGGTCT
GGGACAGACTTCACTCTCACCATCAGCAGACTGGAGCCTGAAGATTTTGCAGTGTAT
TACTGTCAGCAGATGCGTGGTCGGCCGCCGACGTTCGGCCAAGGGACCAAGGTGGAA
ATCAAATCTTCCTCATCGGGTAGTAGCTCTTCCGGCTCATCGTCCAGCGGCGCACATT
ATAATACAGAGATCTTGAAAAGTATTGATAATGAGTGGAGAAAGACTCAATGCATGC
CACGGGAGGTGTGTATAGATGTGGGGAAGGAGTTTGGAGTCGCGACAAACACCTTCT
TTAAACCTCCATCTGTGTCCGTCTACAGATGTGGGGGTTGCTGCAATAGTGAGGGGC
TGCAGTGCATGAACACCAGCACGAGCTACCTCAGCAAGACGTTATTTGAAATTACAG
TGCCTCTCTCTCAAGGCCCCAAACCAGTAACAATCAGTTTTGCCAATCACACTTCCTG
CCGATGCATGTCTAAACTGGATGTTTACAGACAAGTTCATTCCATTATTAGACGT

**Coding nucleotide sequence of KSF-VEGF-C**

GAGGTGCAGCTGTTGGAGTCTGGGGGAGGCTTGGTACAGCCTGGGGGGTCCCTGAGA
CTCTCCTGTGCAGCCTCTGGATTCACCTTTAGCAGCTATGCCATGAGCTGGGTCCGCC
AGGCTCCAGGGAAGGGGCTGGAGTGGGTCTCAGCTATTAGTGGTAGTGGTGGTAGCA

CATACTACGCAGACTCCGTGAAGGGCCGGTTCACCATCTCCAGAGACAATTCCAAGA
ACACGCTGTATCTGCAAATGAACAGCCTGAGAGCCGAAGACACGGCCGTATATTACT
GTGCGAAATCGCCTAAGGTGTCGCTTTTTGACTACTGGGGCCAGGGAACCCTGGTCA
CCGTCTCGAGTGGCGGTAGCGGAGGGTCTGAGCTGACTCAGGACCCTGCTGTGTCTGT
GGCCTTGGGACAGACAGTCAGGATCACATGCCAAGGAGACAGTCTCAGAAGCTATTA
TGCAAGCTGGTACCAGCAGAAGCCAGGACAGGCCCCTGTACTTGTCATCTATGGTAA
AAACAACCGGCCCTCAGGGATCCCAGACCGATTCTCTGGCTCCAGCTCAGGAAACACA
GCTTCCTTGACCATCACTGGGGCTCAGGCGGAAGATGAGGCTGACTATTACTGTAAC
TCCTCTCCCCTGAATCGGCTGGCTGTGGTATTCGGCGGAGGGACCAAGCTGACCGTCC
TAGGCTCTTCCTCATCGGGTAGTAGCTCTTCCGGCTCATCGTCCAGCGGCGCACATTA
TAATACAGAGATCTTGAAAAGTATTGATAATGAGTGGAGAAAGACTCAATGCATGCC
ACGGGAGGTGTGTATAGATGTGGGGAAGGAGTTTGGAGTCGCGACAAACACCTTCTT
TAAACCTCCATGTGTGTCCGTCTACAGATGTGGGGGTTGCTGCAATAGTGAGGGGCT
GCAGTGCATGAACACCAGCACGAGCTACCTCAGCAAGACGTTATTTGAAATTACAGT
GCCTCTCTCTCAAGGCCCCAAACCAGTAACAATCAGTTTTGCCAATCACACTTCCTGC
CGATGCATGTCTAAACTGGATGTTTACAGACAAGTTCATTCCATTATTAGACGT

## Figure S1

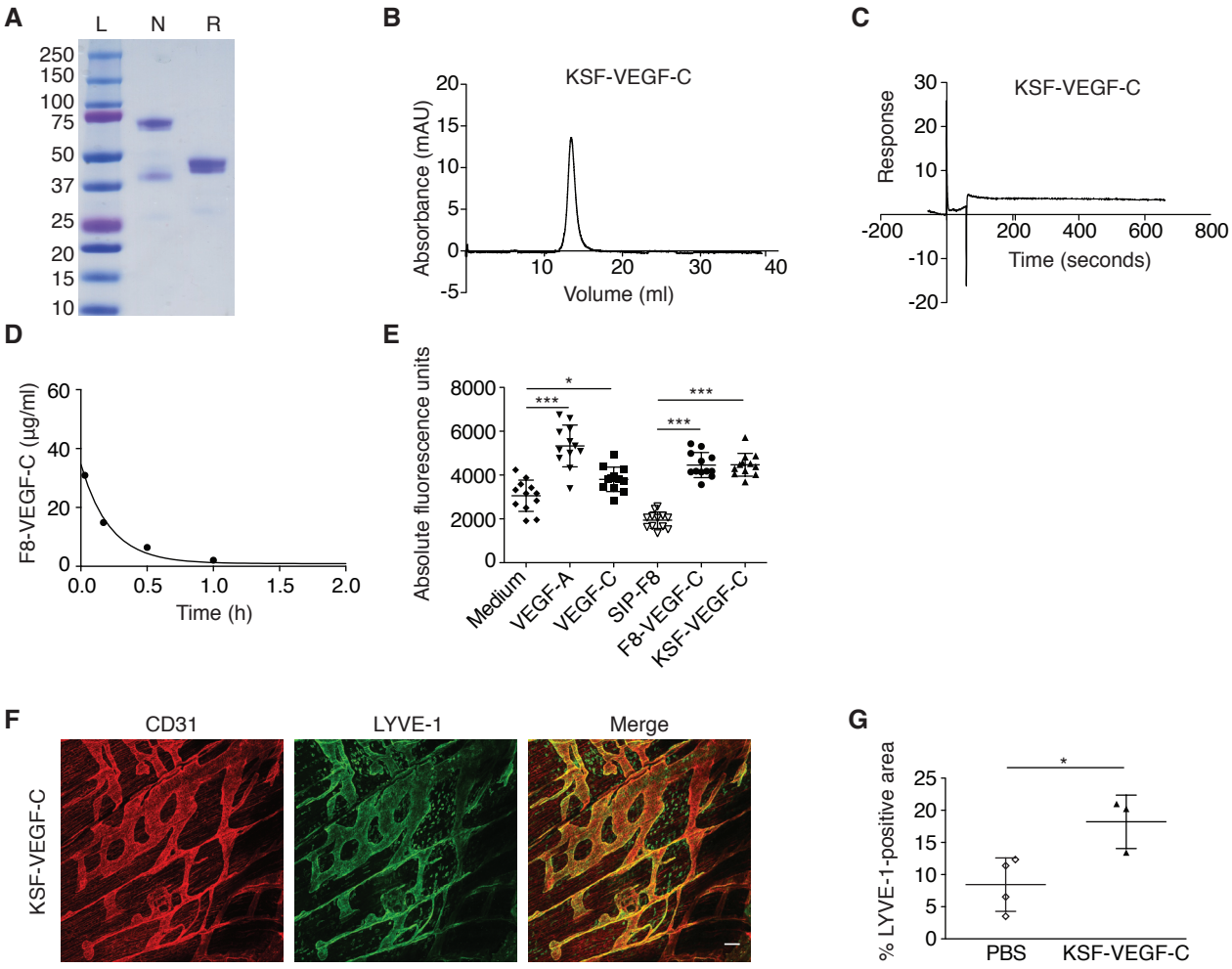


**Figure S1. KSF-VEGF-C is efficiently purified, does not bind EDA and is biologically active. (A)** SDS-PAGE analysis of KSF-VEGF-C. Lanes show size ladder (L), protein under non-reducing (N) or reducing (R) conditions. **(B)** Size-exclusion chromatogram of KSF-VEGF-C. **(C)** Surface plasmon resonance analysis of KSF-VEGF-C using an EDA-coated chip. **(D)** ELISA measurements of serum levels of F8-VEGF-C over time to calculate serum half-life. **(E)** Proliferation assay of human LECs after 72 hours of indicated treatment (n = 12 wells per condition, one-way ANOVA with Bonferroni post-test, one out of three similar experiments shown). **(F)** Whole-mount immunofluorescence staining for CD31 (red) and LYVE-1 (green) on diaphragms of pups having received five injections of PBS or KSF-VEGF-C. Scale bar = 100 µm. **(G)** Quantification of LYVE-1-positive area on stained diaphragm from pups (n = 3-4 animals, two-tailed Student's t-test, one out of two similar experiments shown). Data represent mean ± SD. *P < 0.05, ***P < 0.001.

## Figure S2

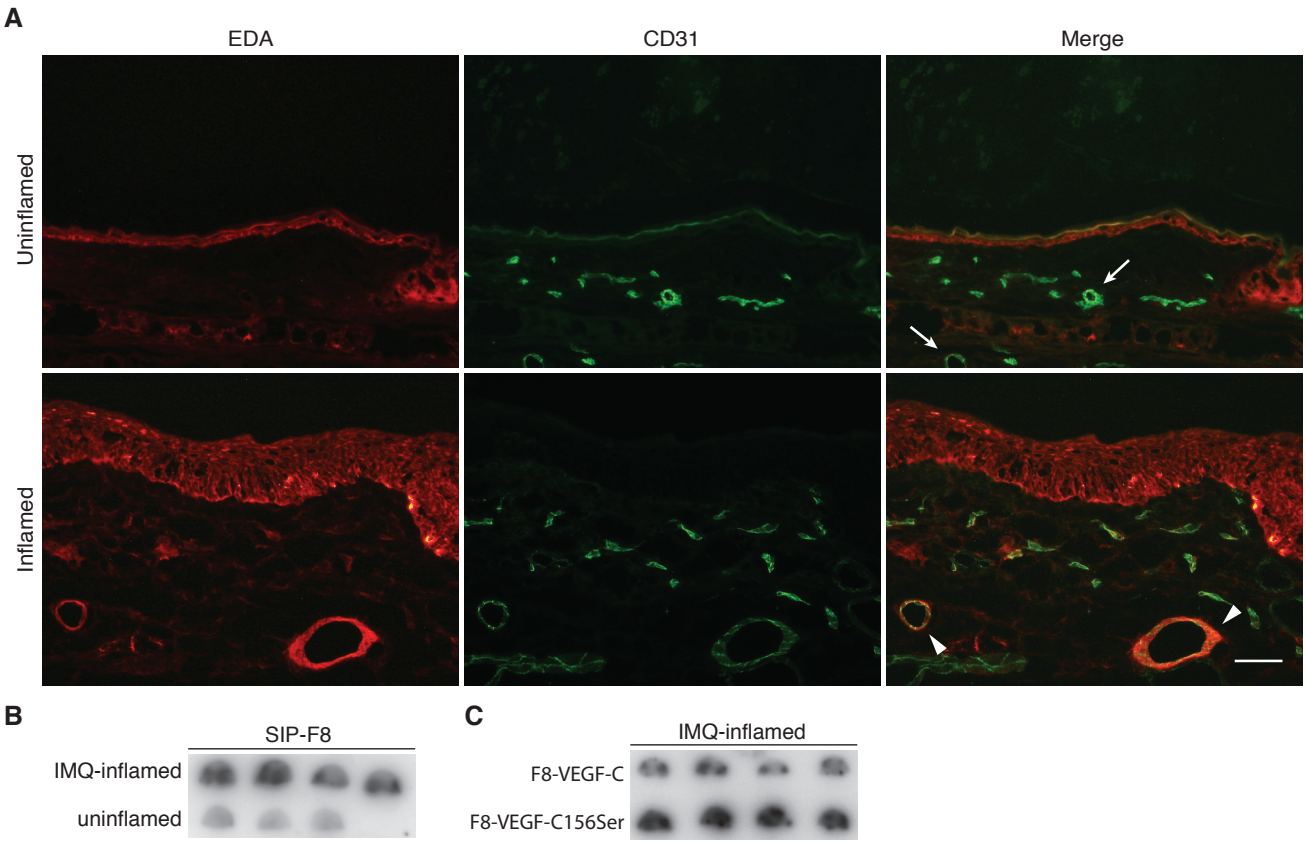


**Figure S2. EDA is expressed in imiquimod-treated but not healthy skin and F8 fusion proteins accumulate in inflamed ear skin. (A)** Immunofluorescence stainings for EDA (red) and CD31 (green) in uninflamed (top) and inflamed (bottom) ear skin of mice treated with imiquimod for seven days (except day six). Scale bar = 100 µm. **(B)** Autoradiography of SIP-F8 in uninflamed and imiquimod-inflamed ears (n = 4 mice per group). **(C)** Autoradiography of F8-VEGF-C and F8-VEGF-C156Ser in inflamed ears (n = 4 mice per group). Arrows: EDA-negative vessels; arrowheads: EDA-positive vessels.

## Figure S3

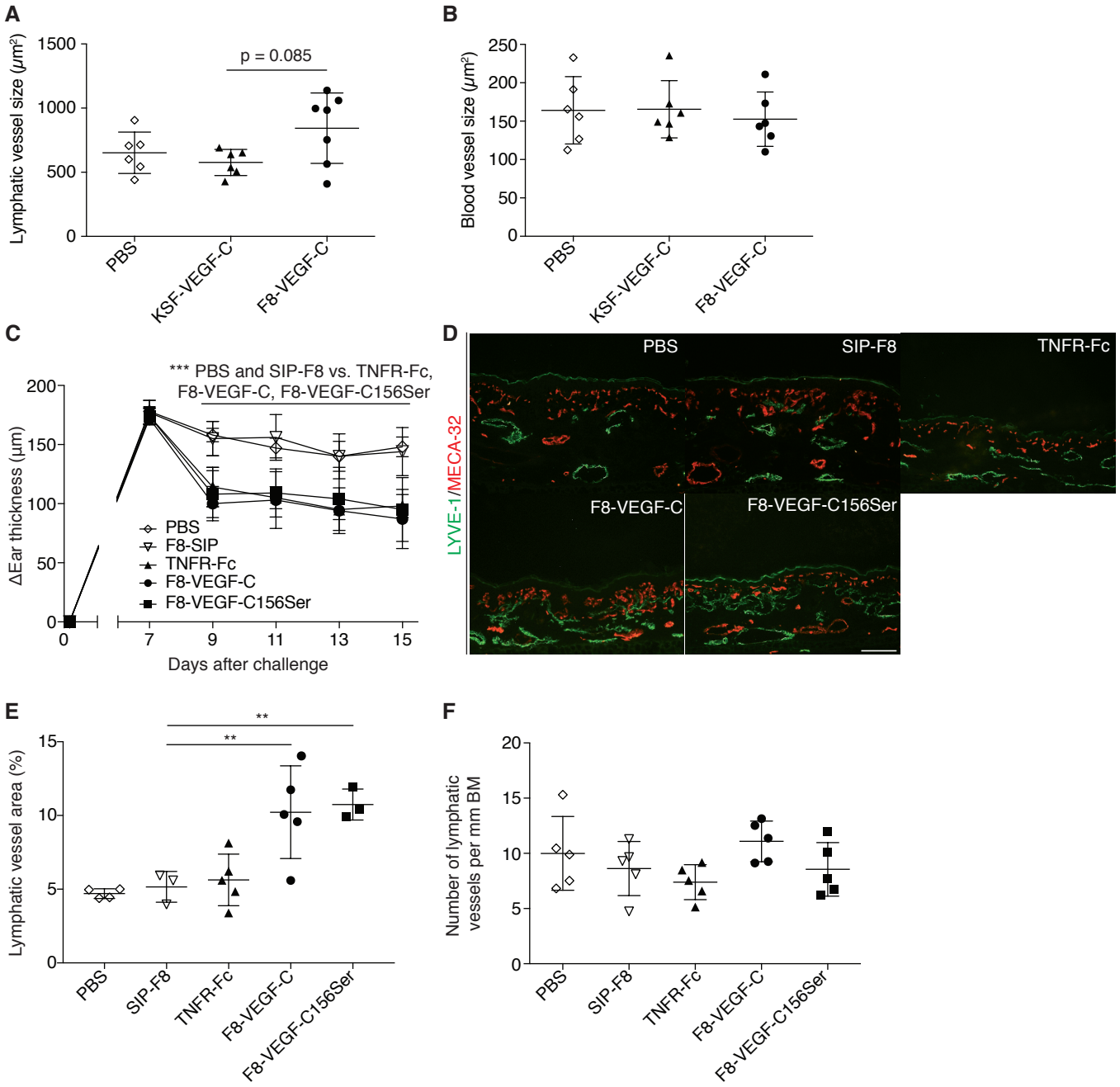


**Figure S3. F8-VEGF-C and F8-VEGF-C156Ser cause lymphatic expansion and alleviate ear inflammation in K14-VEGF-A mice to a degree comparable with TNFR-Fc. (A)** Size of lymphatic vessels in inflamed ears (n = 6-7 animals per group, one-way ANOVA with Bonferroni post-test). **(B)** Size of blood vessels in inflamed ears (n = 6 animals per group, one-way ANOVA with Bonferroni post-test). **(C)** Ear thickness represented as changes compared to ear thickness prior to challenge (n = 5 animals per group, two-way ANOVA with Bonferroni post-test, one out of two similar experiments shown). **(D)** Immunofluorescence images of ears from mice that received the indicated treatment stained for LYVE-1 (green), MECA-32 (red). Scale bar = 100 μm. **(E)** Quantification of lymphatic vessel area (expressed as percent of analyzed area, n = 3-5 animals per group, one-way ANOVA with Bonferroni post-test, one out of two similar experiments shown). **(F)** Number of lymphatic vessels in inflamed ears (normalized to basement membrane, n = 5 animals per group, one-way ANOVA with Bonferroni post-test). Data represent mean ± SD. **P < 0.01, ***P < 0.001.

# Figure S4

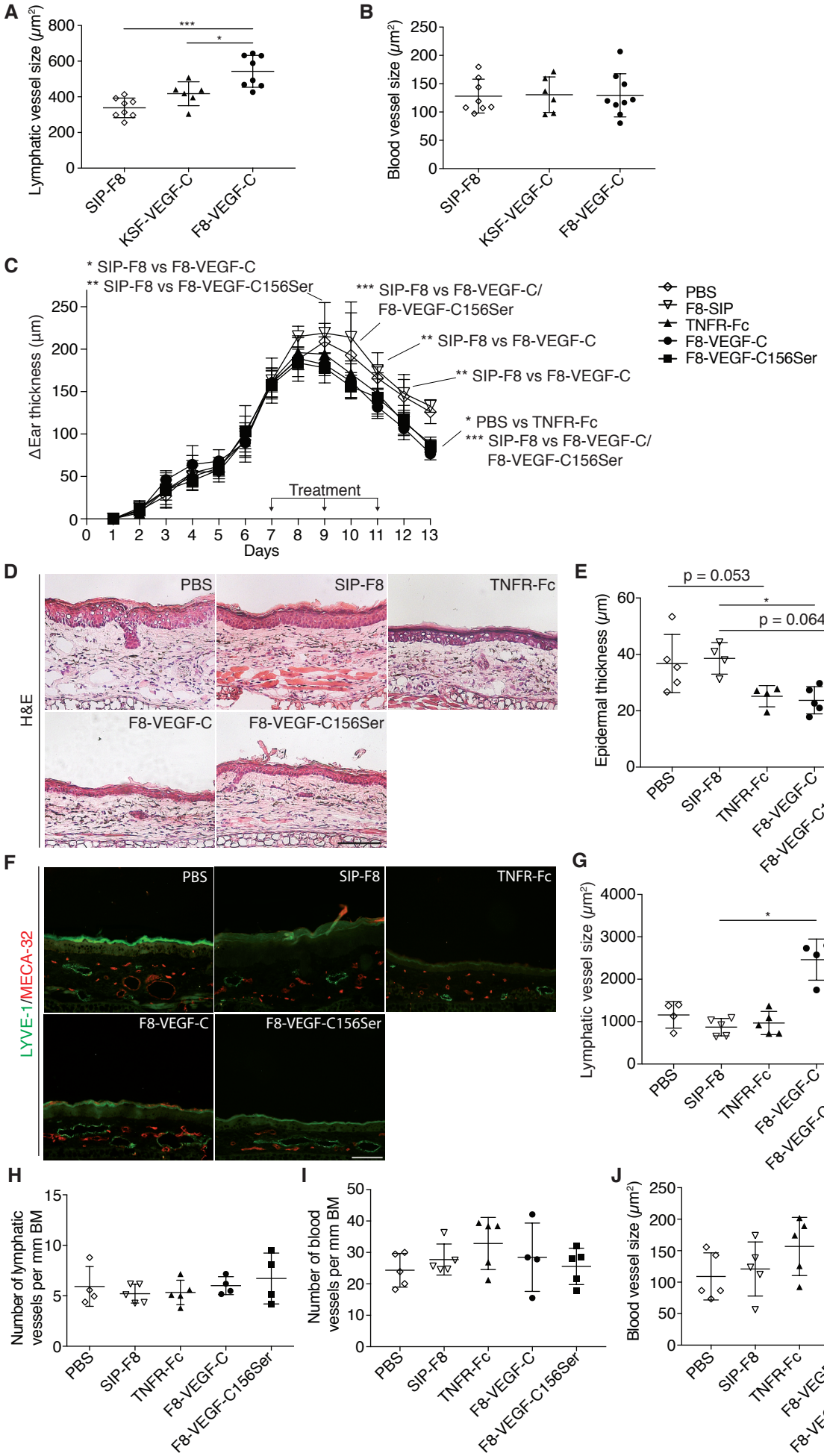
A
Lymphatic vessel size (μm²)
800
600
400
200
0
***
*
SIP-F8
KSF-VEGF-C
F8-VEGF-C
B
Blood vessel size (μm²)
250
200
150
100
50
0
SIP-F8
KSF-VEGF-C
F8-VEGF-C
C
* SIP-F8 vs F8-VEGF-C
** SIP-F8 vs F8-VEGF-C156Ser
*** SIP-F8 vs F8-VEGF-C/
F8-VEGF-C156Ser
** SIP-F8 vs F8-VEGF-C
** SIP-F8 vs F8-VEGF-C
* PBS vs TNFR-Fc
*** SIP-F8 vs F8-VEGF-C/
F8-VEGF-C156Ser
PBS
F8-SIP
TNFR-Fc
F8-VEGF-C
F8-VEGF-C156Ser
ΔEar thickness (μm)
250
200
150
100
50
0
Treatment
0 1 2 3 4 5 6 7 8 9 10 11 12 13
Days
D
H&E
PBS
SIP-F8
TNFR-Fc
F8-VEGF-C
F8-VEGF-C156Ser
E
p = 0.053
*
p = 0.064
Epidermal thickness (μm)
60
40
20
0
PBS
SIP-F8
TNFR-Fc
F8-VEGF-C
F8-VEGF-C156Ser
F
LYVE-1/MECA-32
PBS
SIP-F8
TNFR-Fc
F8-VEGF-C
F8-VEGF-C156Ser
G
*
Lymphatic vessel size (μm²)
4000
3000
2000
1000
0
PBS
SIP-F8
TNFR-Fc
F8-VEGF-C
F8-VEGF-C156Ser
H
Number of lymphatic vessels per mm BM
15
10
5
0
PBS
SIP-F8
TNFR-Fc
F8-VEGF-C
F8-VEGF-C156Ser
I
Number of blood vessels per mm BM
50
40
30
20
10
0
PBS
SIP-F8
TNFR-Fc
F8-VEGF-C
F8-VEGF-C156Ser
J
Blood vessel size (μm²)
250
200
150
100
50
0
PBS
SIP-F8
TNFR-Fc
F8-VEGF-C
F8-VEGF-C156Ser

**Figure S4. F8-VEGF-C and F8-VEGF-C156Ser cause lymphatic expansion and accelerate edema resolution in imiquimod-inflamed mice to a degree comparable with TNFR-Fc. (A)** Size of lymphatic vessels in inflamed ears (n = 6-8 animals per group, one-way ANOVA with Bonferroni post-test). **(B)** Size of blood vessels in inflamed ears (n = 6-9 animals per group, one-way ANOVA with Bonferroni post-test). **(C)** Ear thickness represented as change compared to ear thickness on day 1 (n = 5 animals per group, two-way ANOVA with Bonferroni post-test). **(D)** Hematoxylin and eosin-stained ears of mice having received the indicated treatment. Scale bar = 100 μm. **(E)** Quantification of epidermal thickness on hematoxylin and eosin-stained ear sections (n = 4-5 mice per group, one-way ANOVA with Bonferroni post-test). **(F)** Immunofluorescence images of ears from mice that received the indicated treatment stained for LYVE-1 (green) and MECA-32 (red). Scale bar = 100 μm. **(G)** Quantification of lymphatic vessel size (n = 4-5 animals per group, one-way ANOVA with Bonferroni post-test). **(H)** Number of lymphatic vessels in inflamed ears (normalized to basement membrane length, n = 4-5 animals per group, one-way ANOVA with Bonferroni post-test). **(I)** Number of blood vessels in inflamed ears (normalized to basement membrane, n = 4-5 animals per group, one-way ANOVA with Bonferroni post-test). **(J)** Blood vessel size as quantified in inflamed ears (normalized to basement membrane, n = 4-5 animals per group, one-way ANOVA with Bonferroni post-test). Data represent mean ± SD. *P < 0.05, **P < 0.01, ***P < 0.001.

## Figure S5

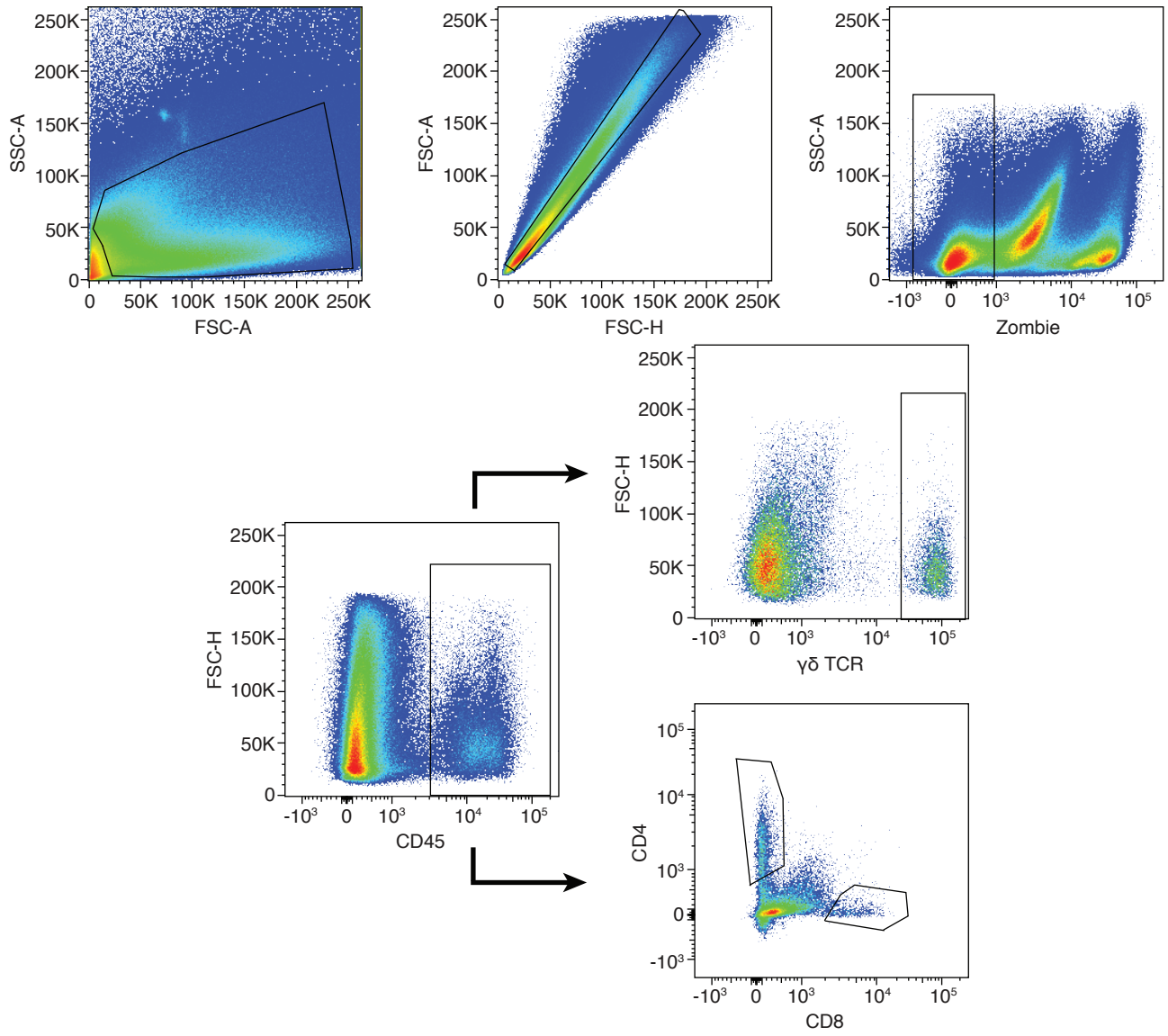


**Figure S5. Gating strategy for analysis of T cell subsets.** Ears of K14-VEGF-A mice at day 15 after challenge were harvested and digested. Stained single cell suspensions were recorded and gated for cells and single cells. Alive single cells were selected for CD45-positivity. $CD45^+$ cells were analyzed with regards to γδ TCR and CD4 as well as CD8 expression. Gates were set based on isotype controls (except for CD45).